INSTITUTE OF PHYSICS PUBLISHING JOURNAL OF PHYSICS B: ATOMIC, MOLECULAR AND OPTICAL PHYSICS

J. Phys. B: At. Mol. Opt. Phys. **36** (2003) 2053–2071 PII: S0953-4075(03)59012-5

The resonance structures of electron interaction with Sr and Ba atoms: low-energy electron scattering and photodetachment of the negative ions

Jianmin Yuan

Department of Applied Physics, National University of Defence Technology, Changsha 410073, People's Republic of China

Received 25 January 2003, in final form 21 March 2003
Published 6 May 2003
Online at stacks.iop.org/JPhysB/36/2053

Abstract

The resonance and near-threshold structures of low-energy electron interaction with Sr and Ba atoms have been investigated by carrying out respectively 11-state and 21-state close-coupling calculations within the *R*-matrix scheme. Part of the core–valence correlation is included by exciting one core electron to the valence orbitals. Results for the low-energy electron scattering and the photodetachment of the negative ions are presented. For Sr, the results show that there is a ^{2}D shape resonance around 0.8 eV above the elastic scattering threshold and a remarkable structure just above the first ^{3}P^o excitation threshold. For Ba, two ^{2}D shape resonances are predicted, just above the elastic scattering threshold and the ^{3}D excitation threshold, respectively.

1. Introduction

Low-energy electron interaction with alkaline-earth atoms has been extensively studied in the past decade. The growing interest in the study of electron scattering with alkaline-earth atoms and the photodetachment of alkaline-earth negative ions has been stimulated by the discovery that one of these closed-shell atoms forms stable negative ions [1, 2]. The studies include the binding energies of the negative ions [3–14], low-energy electron collisions with alkaline-earth atoms [15–25] and the photodetachment of the very loosely bound alkaline-earth negative ions [26–34]. Among those studies, only a few of them concerned low-energy electron interaction processes with Sr and Ba atoms. The only measurement for the absolute value of the scattering cross sections of low-energy electrons from Sr and Ba atoms is due to Romanyuk *et al* [17]. However, independent studies [20, 24] showed that a systematic error was most likely involved in their experiment. For the photodetachment, the only experimental result was obtained recently by Kristensen *et al* [28] for the negative ions of Ca and Sr. There are no experimental results for the photodetachment of the negative Ba ions found in the literature.

As for theoretical studies, a variety of methods have been used to calculate the scattering process of low-energy electrons from Sr and Ba atoms [15, 20, 22–24]. Nevertheless,

0953-4075/03/102053+19$30.00

considerable approximations are still involved in even the most recent result. For the photodetachment process, the theoretical calculations are much less extensive. The only calculation presented in the literature was carried out by Gribakin *et al* [30], and a less complete result was given by Yuan in a post section of a conference [31]. In the work of Gribakin *et al*, the bound state wavefunction of the negative ion was obtained by solving the Dyson equation to include the correlation effect. The reliability of the theory was, however, weakened by using a Hartree–Fock approximation to describe the continuum wavefunction of the free electron. Though the result of Yuan was obtained by solving the close-coupling equation using the R-matrix method, there is still space to improve the accuracy of the target state wavefunctions. Many authors have investigated the binding energy of the negative alkaline-earth ion. In a extensive multiconfiguration Hartree–Fock (MCHF) calculation, Fischer [3] arrived at the correct limit of a valence-only (VO) calculation. Meanwhile, it was shown that the calculated electron affinity of Sr^- and Ba^- is reduced considerably when the core–valence (CV) correlation is considered [11]. We have also shown that the CV correlation has considerable effects on the very low-energy electron scattering from calcium atoms [34].

In the present study, resonance and near-threshold structures of low-energy electron interaction with Sr and Ba atoms will be investigated by carrying out respectively 11-state and 21-state close-coupling calculations within the R-matrix scheme. Part of the CV correlation is included by exciting one core electron to the valence orbitals. Accurate excitation thresholds of the low-lying excited states included in the close-coupling expansion make it possible that the predicted structures can be applied in the identification of the experimental findings. Results for the low-energy electron scattering with the neutral atoms and the photodetachment of the negative ions will be presented.

2. Method of calculation

The R-matrix method for electron–atom and photon–atom interactions has been discussed in great detail by Burke *et al* [35]. The present calculations have been carried out by using the latest Belfast atomic R-matrix codes [36]. In an R-matrix calculation, the wavefunction of the $N + 1$ electron system is given the form

$$\Psi_k(X_1 \dots X_{N+1}) = \hat{A} \sum_{ij} c_{ijk} \Phi_i(X_1 \dots X_N \hat{\boldsymbol{r}}_{N+1} \sigma_{N+1}) u_{ij}(r_{N+1}) + \sum_j d_{jk} \phi_j(X_1 \dots X_{N+1}) \tag{1}$$

where $\hat{A}$ is the antisymmetrization operator to take the exchange effect between the target electrons and the free electron into account. X_i stands for the spatial ($\boldsymbol{r}_i$) and the spin (σ_i) coordinates of the ith electron. The functions $u_{ij}(r)$ under the first sum construct the basis sets for the continuum wavefunctions of the free electron, and Φ_i are the couplings between the target states and the angular and spin parts of the free electron. The correlation functions ϕ_j in the second sum are constructed by the square integrable orbitals to account for the correlation effects not adequately considered because of the cut-off in the first sum. The square integrable orbitals are cast as linear combinations of Slater-type orbitals,

$$P_{nl} = \sum_j C_{jnl} r^{I_{jnl}} \exp(-\xi_{jnl} r), \tag{2}$$

in which the number of Slater-type orbitals necessary to sufficiently approximate these orbitals, P_{nl}, increases as the number of spherical nodes of P_{nl} becomes larger. The pertinent parameters and coefficients, C_{jnl}, of the core orbitals (1s, 2s, 2p, 3s, 3p, 3d, 4s and 4p for Sr; 1s, 2s, 2p, 3s,

3p, 3d, 4s, 4p, 4d, 5s and 5p for Ba) are nearly identical with those of the Hartree–Fock orbitals of the ground states of the corresponding atoms. The valence and pseudo-orbitals (5s, 5p, 4d, $\overline{6s}$, $\overline{6p}$, $\overline{5d}$ and $\overline{4f}$ for Sr; 6s, 6p, 5d, $\overline{7s}$, $\overline{7p}$, $\overline{6d}$ and $\overline{4f}$ for Ba) are optimized independently by using the proven CIV3 computer code [37] to fit the energy levels of the low-lying excited states of the corresponding neutral atoms.

To start the optimization procedure, the initial forms of the above valence and pseudo-orbitals are chosen to be the one-configuration Hartree–Fock results. In the following multiconfigurational calculations, the valence orbitals are used to minimize the ground state energy and to fit the corresponding low-lying excitation levels and the pseudo-orbitals to minimize the energies of the ground state.

The procedure is repeated to arrive at a self-consistent result. The final forms of valence orbitals are not very far from the initial ones, while pseudo-orbitals are significantly different from the corresponding valence orbitals. The bar over the orbital symbols indicates their pseudo-orbital characteristics. Generally speaking, the first sum in equation (1) runs over an infinite number of excited bound states and continuum states of the atom [38]. In order to make the calculations manageable, some pseudo-states are often included to account for the effects of the highly excited states and continuum states approximately [38]. Though in the present case the orbitals with a bar over are included to improve the target states, they can include the effects of continuum states in part. For the intermediate-energy processes many more pseudo-orbitals must be included carefully in order to treat the excitation or ionization processes efficiently, but for the very low-energy processes it is not necessary.

In the close-coupling calculations, an R-matrix radius of 200 au was chosen to ensure that the wavefunction of the very weakly bound electron is completely wrapped within the R-matrix sphere. In forming the $(N + 1)$-electron configurations in equation (1), all possible excitations of the two 5s (or 6s for Ba) valence electrons and a 4p (or 5p for Ba) core electron, which takes the main part of the CV correlation into account, into any of the valence and pseudo-orbitals are allowed, to only exclude the possibility of having more than two electrons in the $\overline{4f}$ orbital. This rule is also applied to the calculation of the atomic eigenstates. As for the construction of the continuum states, each of the angular momentum orbitals is expressed as a linear combination of 80 numerical basis functions.

Two independent optimization procedures have been carried out for each of the atoms. One is CV correlated by exciting one 4p (or 5p for Ba) electron to the valence and pseudo-orbitals. The other one is a VO calculation without any excitation of electrons from the core orbitals. These two independent optimization procedures result in differences in the one-electron orbitals. The calculated atomic energy levels are listed in table 1 compared with the experimental data [39, 40]. Only the ground state and six low-lying excited states of Sr and the ground state and ten low-lying excited states of Ba are presented in the table. There are also four higher-lying pseudo-states of Sr and ten higher-lying pseudo-states of Ba, which are also included in the close-coupling equations but not presented in the table. The accuracy of the calculated excitation energies is quite essential for reasonable predictions of the near-threshold behaviour of the cross sections of electron scattering and photodetachment. One can find that the positions of the low-lying excited states have been predicted quite close to the experimental data. The difference between the theory and experiment is less than 5% for the first few low-lying states of both Sr and Ba atoms. These states are just in the energy region we are interested in most in the present study. The ground state energies of -3131.5942 and -7883.5706 au are obtained for Sr and Ba atoms respectively with the CV correlation, and -3131.5688 and -7883.5495 with the VO correlation. The values of the CV correlated results are very close to those calculated by Sundholm [11] using a finite-element MCHF method with the CV correlations.

Table 1. Calculated relative positions (in electronvolts) of the low-lying excited states of Sr and Ba included in the close-coupling equations compared with experimental values.

Sr	State	Theory		Experiment
	^{1}S	0.0(−3131.5942)[a]	0.0(−3131.5687)[b]	0.0[c]
	^{3}P^o	1.8009	1.8248	1.8229
	^{3}D	2.1765	2.3226	2.2632
	^{1}D	2.4411	2.5045	2.4983
	^{1}P^o	2.7258	2.8984	2.6903
	^{1}D^o	4.1148	4.2005	4.1940
	^{3}F^o	4.1290	4.1853	4.1726
Ba	State	Theory		Experiment
	^{1}S	0.0(−7883.5706)[a]	0.0(−7883.5495)[b]	0.0[c]
	^{3}D	1.1604	1.1604	1.1601
	^{1}D	1.4325	1.3340	1.4129
	^{3}P^o	1.6141	1.4998	1.6221
	^{1}P^o	2.2984	2.3624	2.2392
	^{1}D^o	2.8877	2.8293	2.8609
	^{3}P	2.8905	2.8516	2.9377
	^{1}D	2.9116	2.8131	2.8594
	^{3}F^o	2.9508	2.8671	2.8621
	^{3}D^o	3.3062	3.1539	3.0591
	^{1}S	3.3494	3.2757	3.3175

[a] The present CV correlated result. The number in the parentheses is the ground energy in atomic units.
[b] The present VO correlated result. The number in the parentheses is the ground energy in atomic units.
[c] The experimental data are from [39] except for the second ^{1}S state of Ba, which is from [40].

3. Results and discussion

To start our discussion, we give more details about the calculation of the atomic levels as well as the bound negative ion states. We use a configuration–interaction (CI) wavefunction to describe the atomic ground and excited states appearing in the close-coupling expansion. The radial part of the wavefunction is constructed by using analytic Slater-type basis functions. As mentioned in the above section, the pertinent parameters have been optimized to fit the atomic levels. This is not a simple multiconfiguration Hartree–Fock self-consistent calculation, as we have to get all the excited states in the close-coupling expansion rather than only one of them, for example the first excited state, to fit the true position as closely as possible, and we also have to try to get a ground state energy as low as possible. Therefore, independent optimizations have to be done, respectively, for the CV correlated calculations and the VO calculations. Even then these Slater-type bases are still less suited to describe the rather diffuse loosely bound negative ion states. Fortunately, an algorithm for the bound state has been included in the R-matrix computer code employed in the present calculations. The CI expansion constructed by the analytic Slater-type basis functions for the negative ion state is represented by the second term on the right-hand side of equation (1). It has been mentioned that this CI expansion for the negative ion state is far from sufficient, in particular for the CV correlated calculation. This incompleteness can be improved effectively by the first term of the close-coupling wavefunction of equation (1). An electron affinity of 66 meV for Sr^- and an electron affinity of 183 meV for Ba^- are obtained by our CV correlated calculations,

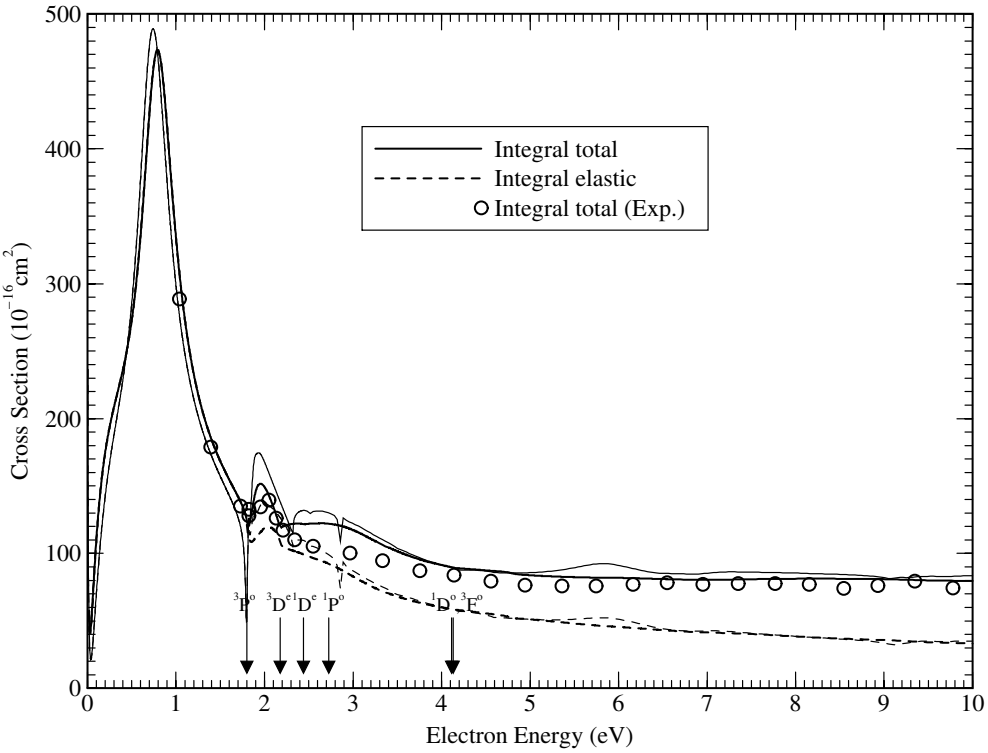

Figure 1. Integral total and elastic cross sections of low-energy electron scattering from ground state Sr atoms. The thick curves represent the CV correlated results, and thin curves the VO results. Open circles represent the experimental points of Romanyuk *et al* [17], which have been shifted systematically to move the threshold structure observed in the experiment to its actual position at 1.82 eV.

which are also in reasonable agreement with the CV correlated results of Sundholm [11]. The corresponding VO electron affinities are 105 and 296 meV for Sr^- and Ba^-, respectively. The reduction of the electron affinity caused by the CV correlation is considerable as also shown by many other authors [11]. The new Belfast *R*-matrix code does not calculate the contributions to the matrix elements from the wavefunctions outside the *R*-matrix sphere, so that we have to choose a large enough *R*-matrix radius of 200 au. In order to make a convergent expansion, up to 80 numerical basis functions for each angular momentum are included in the first term of equation (1).

3.1. Electron scattering from Sr atoms

The early studies on the electron scattering with Sr atoms were summarized by Fabrikant [16] in a review article. The reliability of the early theoretical studies is marred significantly by the less accurate wavefunctions of the atomic states and the insufficient close-coupled collision channels. Therefore, in the present discussion only the experimental result of Romanyuk *et al* [17] for the absolute cross section will be presented together with our calculated result. In figure 1, the integral elastic and total cross sections are presented together with the experimental data of Romanyuk *et al* [17]. The experimental data are for the integral total cross sections and shows some structures. The sharp increase of the cross section with the collision energy going

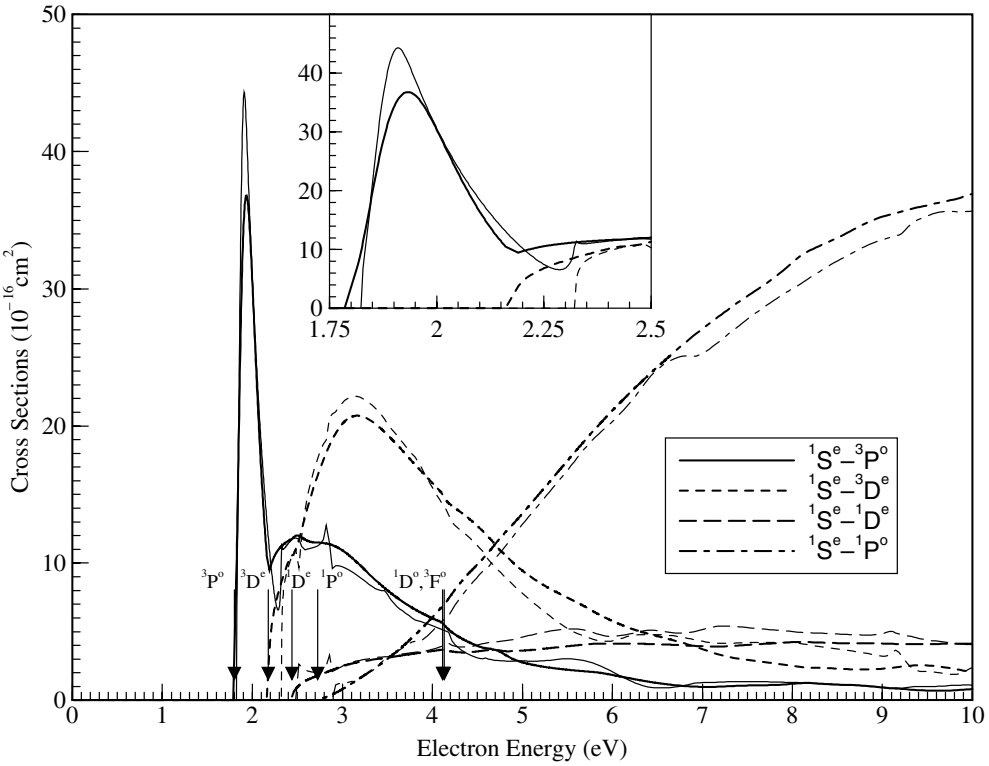

Figure 2. Integral excitation cross sections of low-energy electron scattering from ground state Sr atoms. The thick curves represent the results of CV calculation, while the corresponding thin curves represent the corresponding VO results, as in figure 1.

down was originally attributed to a low-lying ^{2}P shape resonance. The second mini-peak was originally located at 1.2 eV, and explained as a slightly higher-lying ^{2}D shape resonance state. The present results show clearly, however, that the low-lying man peak is caused by a ^{2}D shape resonance state, while the second mini-peak by the threshold effect of the first excited ^{3}P^o state, and its actual position should be slightly above 1.8 eV. Our early results for Ca also indicated that there is most likely a systematic error in the electron energies in their experiment. In order to get a reasonable comparison between theory and experiment, in figure 1 the experimental points of Romanyuk *et al* [17] have been moved systematically by 0.8 eV to higher energies. One can find that the agreement between theory and experiment is quite satisfactory. The corresponding results of the VO calculation are also shown in figure 1 by the thin curves. One can find that a slight shift of the ^{2}D shape resonance peak exists between the thick and thin curves. More apparent differences are shown just above the first excitation threshold. At the energies above 5 eV, the so-called CV correlation has little effect.

In figure 2, the integral excitation cross sections from the ground state to the first four low-lying excited states are presented. One can see that the excitation cross section to the first ^{3}P^o excited state makes a significant contribution to the second mini-peak observed in the experiment. The excitation to the ^{1}P^o excited state makes the main contribution to the inelastic processes at the energies above 6 eV, and below this energy the excitations to ^{3}P^o, ^{3}D, ^{1}D and ^{1}P^o excited states make comparable contributions. The inelastic excitations to both ^{1}D^o and ^{3}F^o states are very weak and the cross sections are not shown in figure 2. Contributions of up to

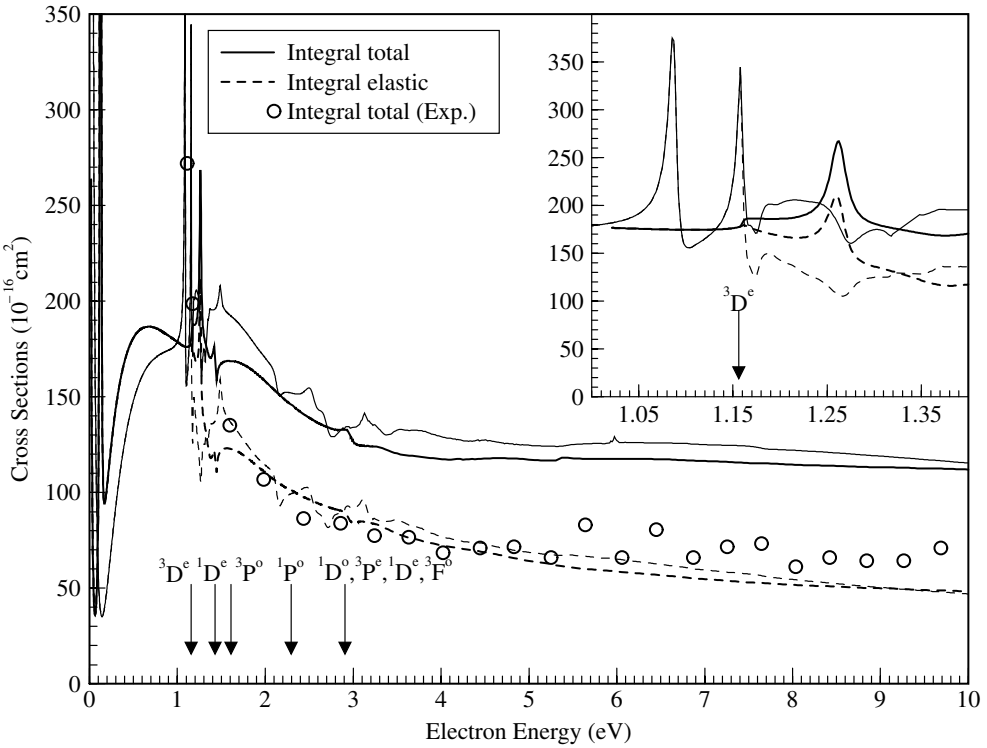

Figure 3. Integral total and elastic cross sections of low-energy electron scattering from ground state Ba atoms. The meanings of the thick and thin curves are the same as in figure 1. Open circles represent the experimental points of Romanyuk *et al* [17], which have been shifted systematically with the same energy as in figure 1.

26 partial waves have been included in both elastic and excitation cross sections. Considerable changes caused by taking more correlations are only found for the excitation cross sections just above the first excitation threshold, where a sharp cusp is produced.

3.2. Electron scattering from Ba atoms

In figure 3, the cross sections of slow electron collision with Ba atoms are presented, which include integral total and elastic cross sections. The experimental points of the integral total cross section of Romanyuk *et al* [17] are also plotted in figure 3 for comparison. As the order of the low-lying excited states of Ba is different from that of Sr, the structures of the energy dependence of the cross sections of Ba have different characteristics from those we plotted in figure 1 for Sr. We have two very sharp peaks at respectively 0.122 and 1.26 eV and a broad maximum from 0.5 to 3 eV. Both of the two sharp peaks come from the ^{2}D partial wave and have the typical shape resonance features. The first one is just above the elastic scattering threshold and is associated with the collision channel ^{1}S + kd and the second one just above the excitation threshold of the first excited ^{3}D state and associated with the collision channel ^{3}D + kd. The broad maximum from 0.5 to 3 eV comes from the contributions of ^{2}S, ^{2}P^o and ^{2}F^o partial waves, and does not reflect any resonances.

The cross sections obtained with the VO correlation are also displayed in figure 3 for Ba. Compared to the case of e–Sr scattering, CV correlation has much more significant influences

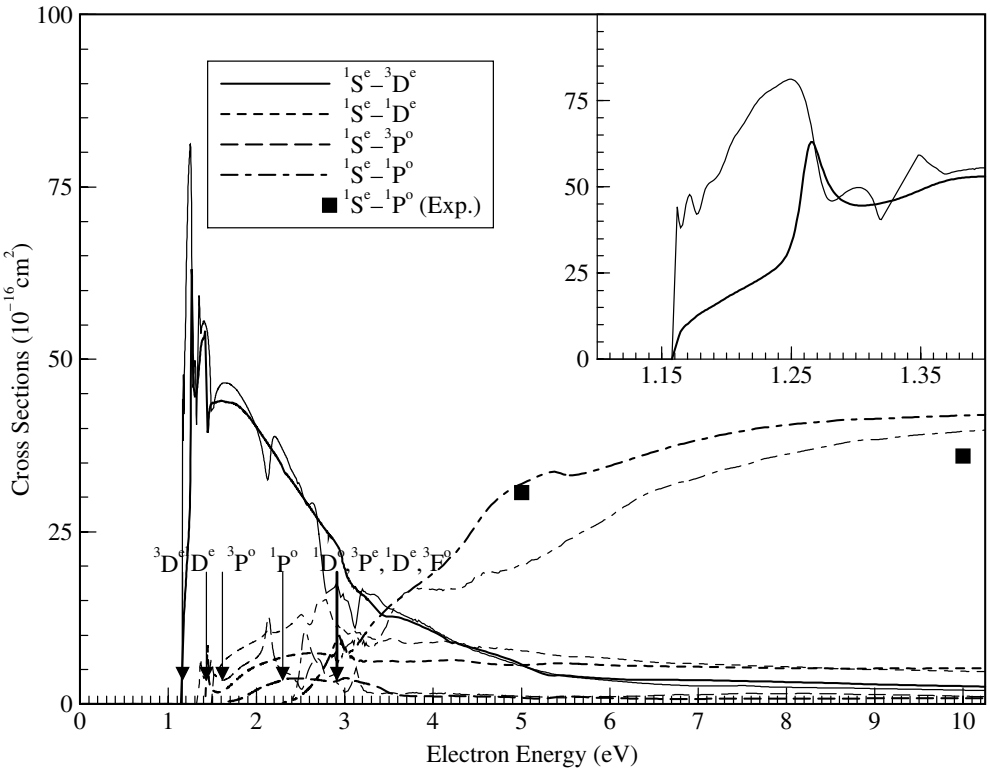

Figure 4. Integral excitation cross sections of low-energy electron scattering from ground state Ba atoms. The meanings of the thick and thin curves are the same as in figure 2. The filled squares represent the experimental points of Wang *et al* [42].

on the cross sections of electron scattering with Ba atoms. A very low-lying ^{2}D wave shape resonance is also predicted at a lower energy, 0.043 eV, and the cross sections from 0.2 to 1.0 eV also show considerable difference between the CV and VO calculations. The most drastic change from CV to VO results occurs around the first excitation threshold. Without the CV correlation, the ^{2}D resonance peak predicted by the CV calculation around 1.26 eV just above the ^{2}D excitation threshold, as a shape resonance, moves to 1.09 eV just below the ^{2}D excitation threshold, as a Feshbach resonance. The VO calculation also predicts a second sharp structure just across the ^{2}D threshold. This structure is a typical cusp caused by the so-called threshold effect of the s-wave scattering [41] and reaches its top just at the threshold. The movement of the ^{2}D resonance peak from 1.26 eV in the CV results to 1.09 eV in the VO results can be explained as follows. From the above discussions about electron affinity, we know that CV correlation reduces the electron affinity of Ba^- by about 113 meV. This is equivalent to moving the ground state energy of the neutral atom to a lower position relative to the ground state energy of the negative ion. That also means that the positions of the first few excited states of the neutral atom would move to lower energies by approximately the same amount relative to the structures of the $(N + 1)$-electron system. The movement of the ^{2}D resonance structure from CV to VO calculations is 170 meV and comparable to the 110 meV reduced in the electron affinity by the CV correlations.

Comparison with the experimental data shows considerable distance between theory and experiment. As in the case of figure 1, the experimental points plotted in figure 3 have been

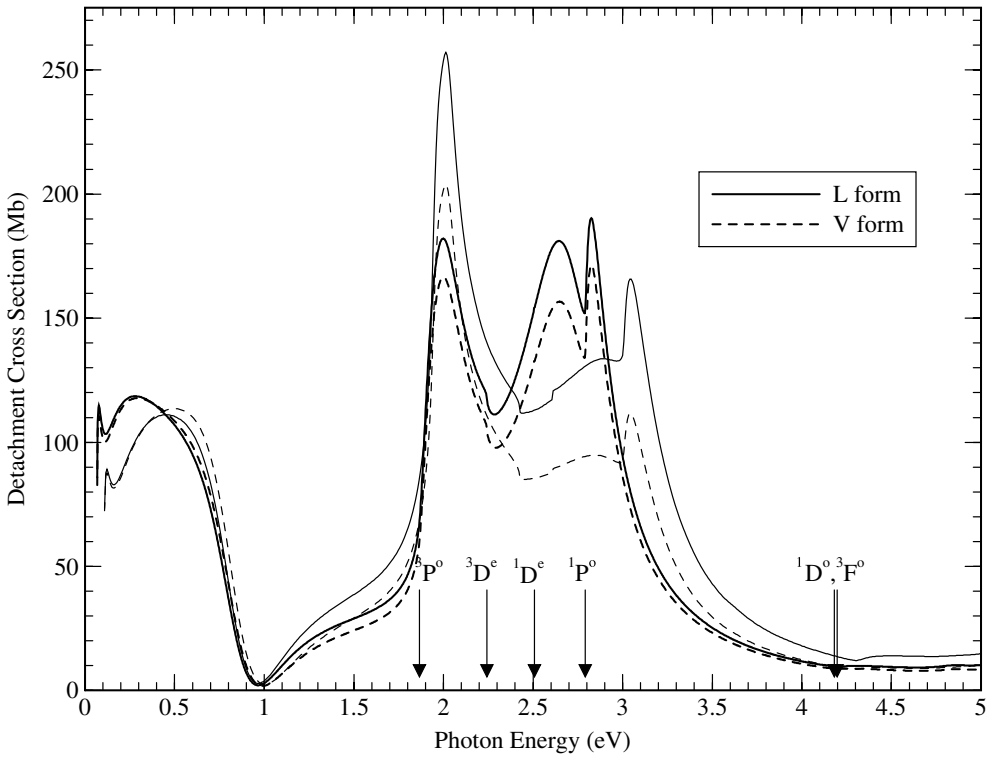

Figure 5. Total photodetachment cross sections of Sr^- ions. Both length (solid curves) and velocity (dashed curves) forms of the present results are presented. The thick and thin curves are also used to distinguish the CV correlated and the VO calculations, as in figure 1.

moved systematically by 0.8 eV to higher energies. One can find that the absolute values of the total cross sections above 1.5 eV have been predicted to be much higher than the corresponding experimental points and the agreement between theory and experiment is much poorer than that for the Sr atom. We attribute this to the relativistic effects, which have been completely ignored in the present studies.

In figure 4, the excitation cross sections from the ground state of the Ba atom to the first four excited states are presented. Two experimental points [42] for the excitation from ground to the $^1P^o$ excited state are also plotted for comparison. One can find that, due to the channel coupling, a sharp peak caused by the shape resonance just above the first excitation threshold also appears in the excitation cross section from the ground to the ^3D excited state. One can also find that the excitation cross sections from ground to the $^1P^o$ excited state are calculated in quite good agreement with the experimental points. As in the case of the Sr atom, the excitation to the $^1P^o$ state makes the main contribution to the inelastic cross sections in the plotted energy region.

A significant difference occurs too between the CV and VO results for the excitation cross sections nearby the ^3D threshold. The reasons for this large discrepancy are the same as in the total cross section. From the inset window in figure 4, one can see that, although both CV and VO calculations give typical s-wave threshold behaviour for the cross sections just above the ^3D threshold, the VO result shows a much sharper increase, and obeys the Wigner's threshold law within a much shorter energy region, than the CV result.

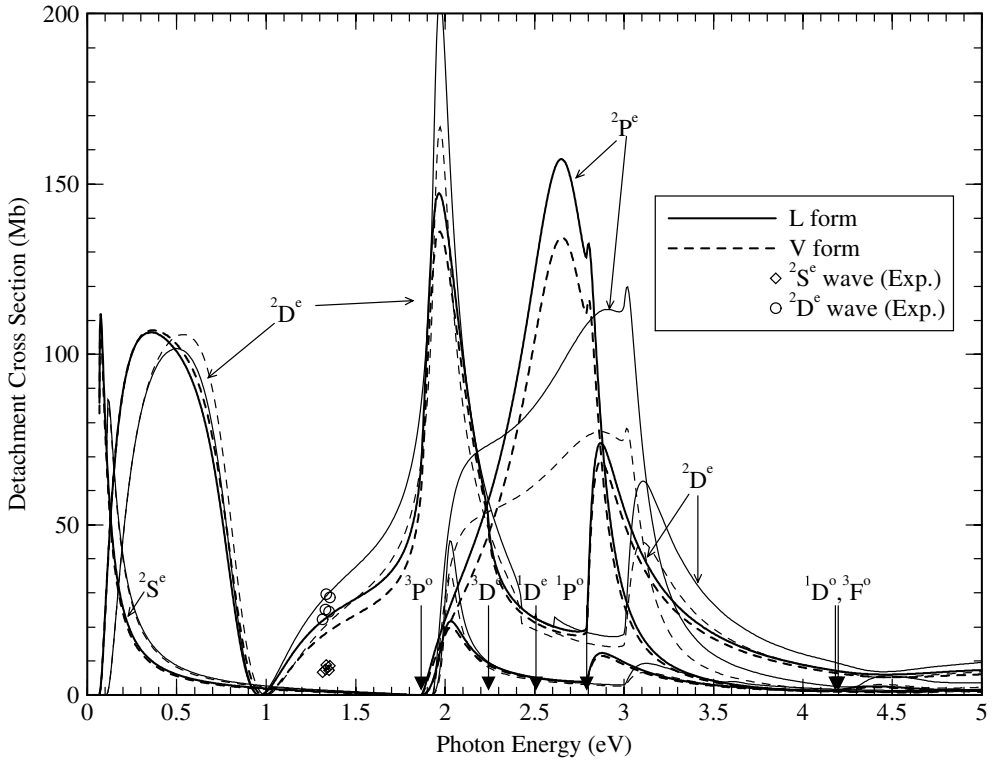

Figure 6. Detailed contributions of the three partial waves to the total photodetachment cross sections of Sr^- ions. The meanings of the curves are the same as in figure 5. The open diamonds and the open circles represent the experimental points of Kristensen *et al* [28].

3.3. Photodetachment of Sr^- ions

In figure 5, the photodetachment cross sections of Sr^- ions are presented with the results of both length and velocity forms, and the agreement between these two forms is reasonably good. Some general threshold features, Cooper minimum and resonance peaks have been shown in the cross section. There is no systematic experimental result for the photodetachment process of Sr^- ions. Kristensen *et al* [28] gave only a few points around the photon energy of 1.3 eV for partial wave expansion cross sections, and these will be discussed and compared with our results in figure 6. As for the comparison with other theories, the only results presented in the literature by other authors are due to Gribakin *et al* [30]. However, as the free electron is only described at a Hartree–Fock level, their calculations only gave the direct photodetachment cross sections, i.e. the elastic channel cross sections, and did not include the channel interactions. Comparison with their $^1S + ks$ ionization channel cross section will be given in figure 7, and $^1S + kd$ ionization channel cross section in figure 9. Adequate descriptions for both bound and continuum wavefunctions are required for a reasonable prediction of the photodetachment process. Our ground state energy of Sr is -3131.5942 au, which is only 0.0078 au higher than the CV correlated MCHF calculation of Sundholm [11]. As argued by Fischer and Hansen [32], and from our early calculation [34] for the photodetachment of Ca^- ions, a description of the neutral target within this range of accuracy should be sufficient, because the photodetachment cross section is not sizably sensitive to the target state but rather to the continuum wavefunction

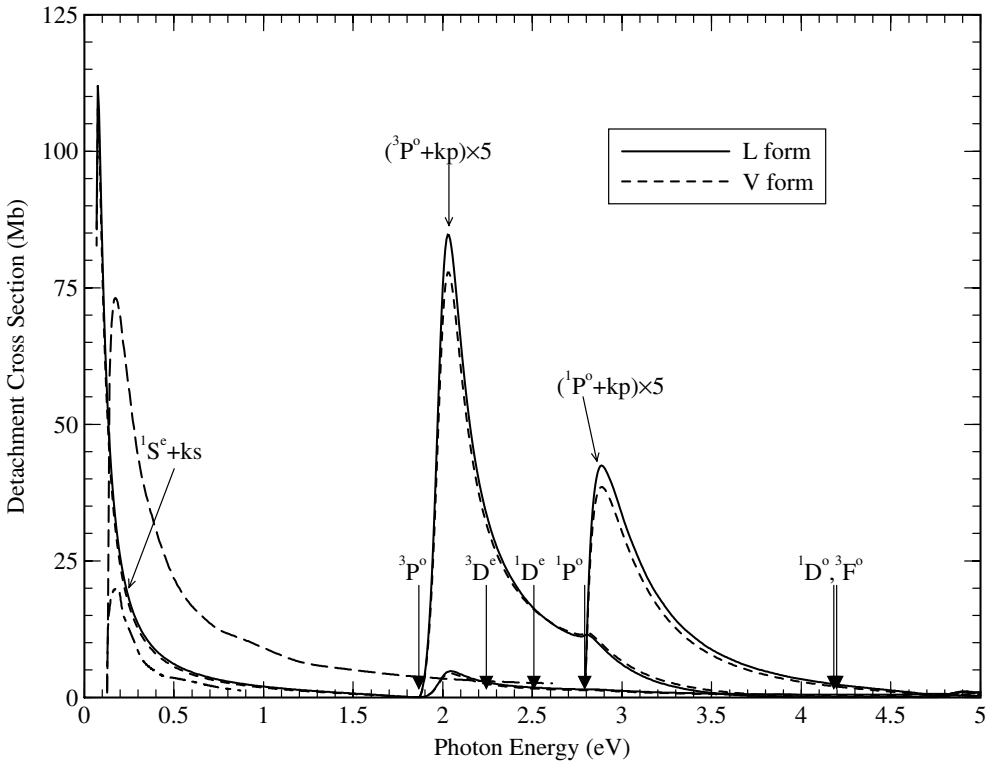

Figure 7. Detailed contributions of the individual ionization channels to the ^{2}S partial wave photodetachment cross sections of Sr^- ions. The meanings of the curves are the same as in figure 5, except that the results of Gribakin *et al* [6] for the ionization channel ^{1}S + *k*s are represented by a long-dashed curve for the length form and a dot–dashed curve for the velocity form.

and that of the extra electron bound to the neutral target. From our calculations, it has also been found that correct excitation energies of the atom are quite essential for an adequate description of the photodetachment process above the Cooper minimum. In the present calculations, not only is the ground state energy minimized, but also the first six excited states are calculated, in good agreement with experiment. The largest error for the six excitation energies is less than 0.087 eV.

The VO result of the total photodetachment cross section of Sr^- ions is also shown in figure 5, by a thin solid curve for the length form, and by a thin dashed curve for the velocity form. The ionization of the VO calculation is about 50 meV larger than the CV calculation, and this results in a apparent discrepancy for the cross sections just above the ionization threshold. The Cooper minima have been predicted very close to each other in the CV and VO results. From 2.0 to 4.0 eV, as the relative heights of the three nearby peaks are predicted quite differently by CV and VO calculations, the total cross sections behave quite differently for CV and VO calculations. The agreement between the length and velocity forms is poor for the VO results.

Partial cross sections are helpful to understand the origins of the structures presented in figure 5. One can see from figure 6, in which the partial cross sections of the photodetachment of Sr^- ions are plotted, that the platform from 1.9 to 2.9 eV is a combined contribution of ^{2}P and ^{2}D symmetries. A much higher peak of the ^{2}D symmetry after the first excitation threshold

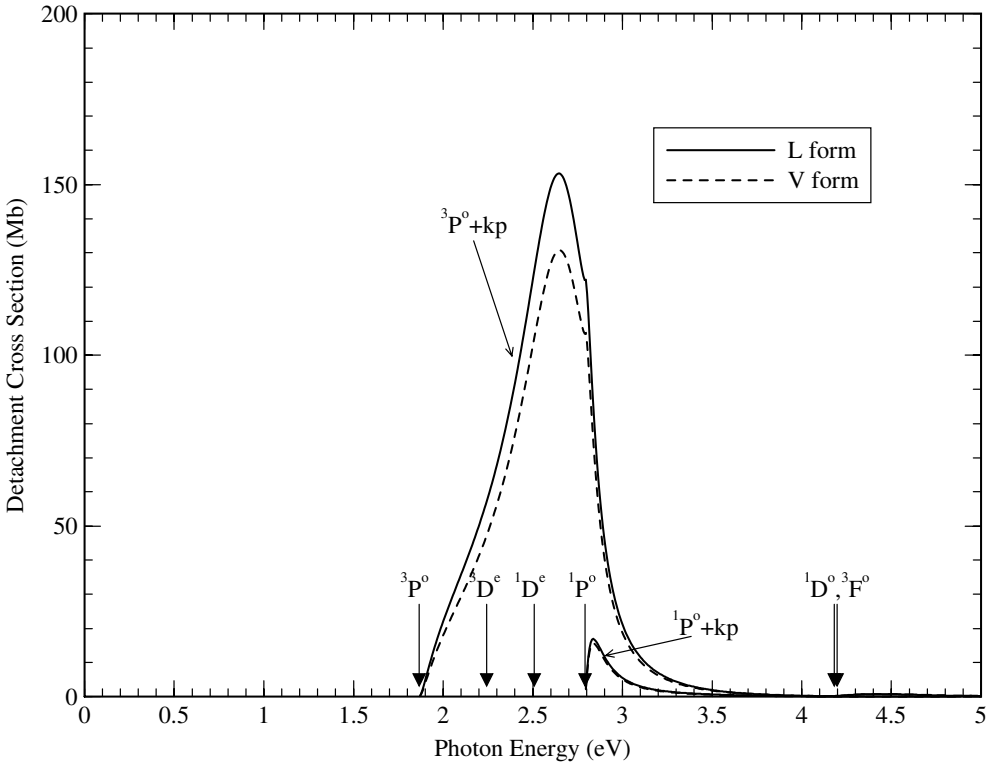

Figure 8. Detailed contributions of the individual ionization channels to the ^{2}P partial wave photodetachment cross sections of Sr^- ions. The meanings of the curves are the same as in figure 5.

reflects the same physical information we saw in figure 2, where a remarkable structure was seen in the total and excitation cross sections of electron scattering between the $^3P^o$ and ^3D thresholds. Experimental points of Kristensen *et al* [28] for the cross sections of the partial waves of ^2S and ^2D are plotted in figure 6 for comparison. For the partial wave ^2D theory goes near the experimental points, while for ^2S the discrepancy between theory and experiment is unacceptable. One possible reason for this larger discrepancy is that the absolute value of this partial wave around 1.3 eV is too small. One can find that the largest changes induced by the CV correlation occur in the ^2P partial cross sections, which are contributed only by the excitation channels.

We have also extracted from our calculation the contributions of the major ionization channels to the three partial cross sections. The result is shown in figures 7–9. As follows from the inspection of figure 7, there are two weak shape resonances related to the ionization channels $(5s5p\ ^3P^o + kp)^2S$ and $(5s5p\ ^1P^o + kp)^2S$. From figure 8, it can clearly be seen that the broad peak of the total cross section at 2.6 eV originates mainly from the contribution of the $(5s5p\ ^3P^o + kp)^2P$ ionization channel. This increase is most likely caused by the interaction between $(5s5p\ ^3P^o + kp)^2P$ and $(5s5p\ ^1P^o + kp)^2P$ channels. Channel contributions to the ^2D partial cross section are displayed at the bottom of figure 9. The cusp around 1.7 eV in the detachment channel $(5s^2\ ^1S + kd)^2D$ and the broad maximum around 2.0 eV of the $(5s5p\ ^3P^o + kp)^2D$ channel reflect the channel interaction and are quite sensitive to the positions of the thresholds of $^3P^o$ and ^3D. From figure 9, it can be seen more clearly that the third

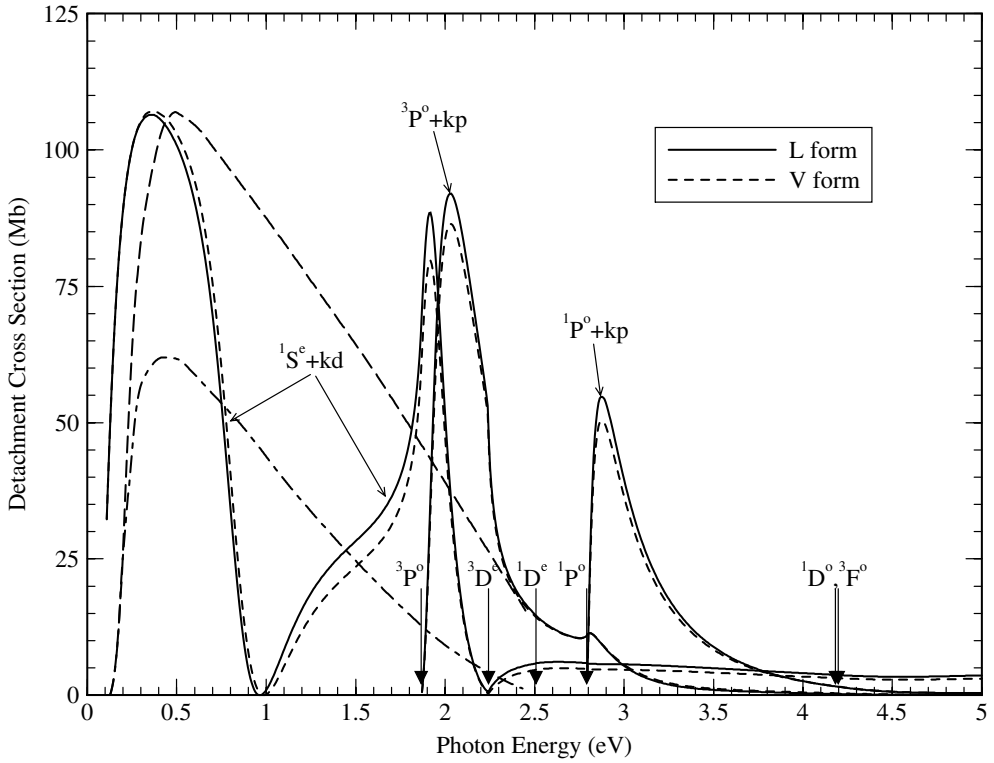

Figure 9. Detailed contributions of the individual ionization channels to the ^{2}D partial wave photodetachment cross sections of Sr^- ions. The meanings of the curves are the same as in figure 5, except that the results of Gribakin *et al* [6] for the ionization channel $^1S + k$d are represented by a long-dashed curve for the length form and a dot–dashed curve for the velocity form.

narrow peak just after the $^1P^o$ excitation threshold is dominated by the shape resonance in the $(5s5p\ ^1P^o + kp)^2D$ detachment channel.

Comparisons with the theoretical results of Gribakin *et al* [30] are made in figures 7 and 9. In figure 7, the cross section of the ionization channel $(5s^2\ ^1S + ks)^2S$ of those authors shows considerable differences from the present results. The differences are mainly caused by the correlations in the descriptions of the ionized electron. In their calculations, the bound electron in the negative ion is well described, with an accuracy comparable to the present study, while the free electron is treated too approximately by a Hartree–Fock wavefunction. They did not consider the coupling among the ionization channels, either. Therefore, they just gave the results for the elastic channel, and the structures observed around the excitation threshold in the present study were completely ignored by them. In figure 9, the cross section of the ionization channel $(5s^2\ ^1S + kd)^2D$ of Gribakin *et al* are shown to compare with our result. The importance of correlations for the free electron can be seen more clearly for this ionization channel. A Cooper minimum is produced near 1.0 eV photon energy when the correlations have been taken into account carefully for both bound and free electrons, while the cross section does not reach its minimum point before 2.5 eV when the correlation is only neglected for the free electron. The Cooper minimum is caused by a cancellation in the integration over the wavefunctions; therefore, it should be more sensitive to the accuracy of the wavefunctions of both bound and free electrons.

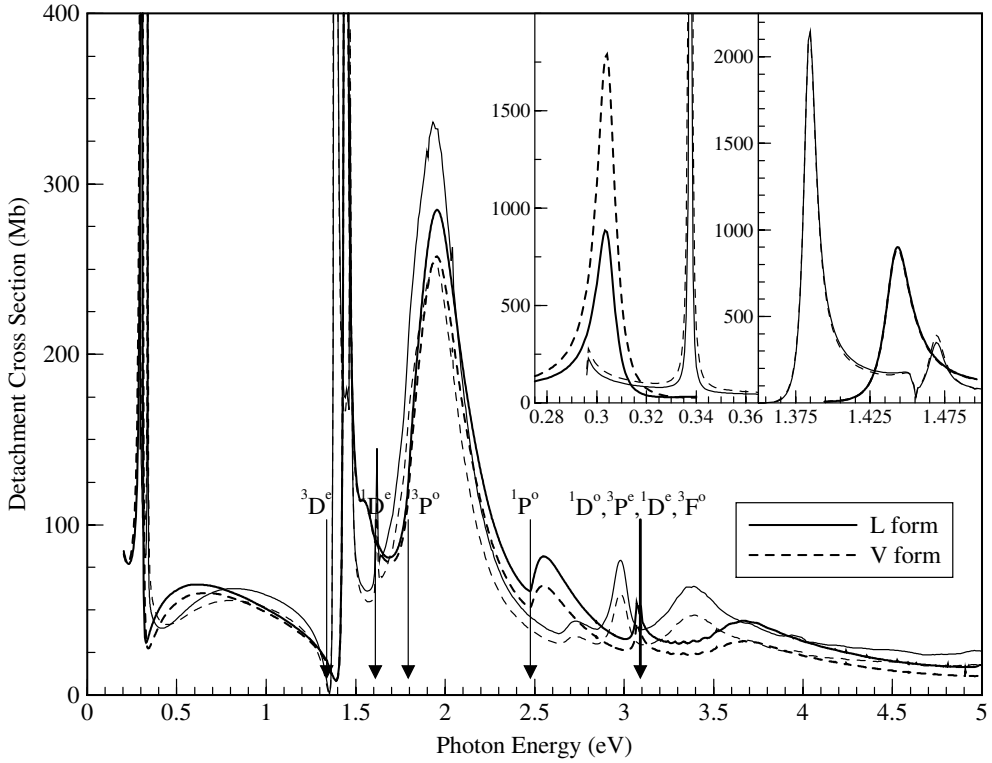

Figure 10. Total photodetachment cross sections of Ba^- ions. The meanings of the curves are the same as in figure 5.

3.4. Photodetachment of Ba^- ions

In figure 10, the photodetachment cross sections of Ba^- ions are presented with the results of the two forms of expression. Agreement between these two forms is reasonably good. As the order of the low-lying excited states of the Ba atom is different from that of the Sr atom and the former investigated atom, Ca [33], the general features, for example distribution of the resonance peaks, or the energy dependence of the photodetachment cross sections, of Ba^- ions are quite different from those shown in figure 5 for Sr^- ions. Two sharp resonance peaks located respectively around 0.3 and 1.45 eV and a few broader and lower peaks have been shown. The so-called Cooper minimum appears at 0.33 eV just above the first shape resonance peak. The accuracy for the descriptions for both bound and continuum wavefunctions is the same as for Sr atoms, except that the relativistic effect should be much more important for Ba atoms. Our ground state energy of Ba is -7883.5706 au, which is only 0.0280 au higher than the CV correlated MCHF calculation of Sundholm [11]. The largest error for the excited states in table 1 is 0.24 eV, and this is only for the higher-lying $^3D^o$ state. For all other states the error is less than 0.05 eV. There is no experimental result available for the photodetachment process of Ba^- ions. Comparison with the theories by Gribakin *et al* [30] will be given in figures 12 and 14 for separate ionization channels.

A qualitative difference between the CV and VO results appears around the first excitation threshold. As in the electron scattering, a Feshbach type resonance peak is predicted by the VO calculation just below the threshold, and a potential type resonance peak by the CV calculation

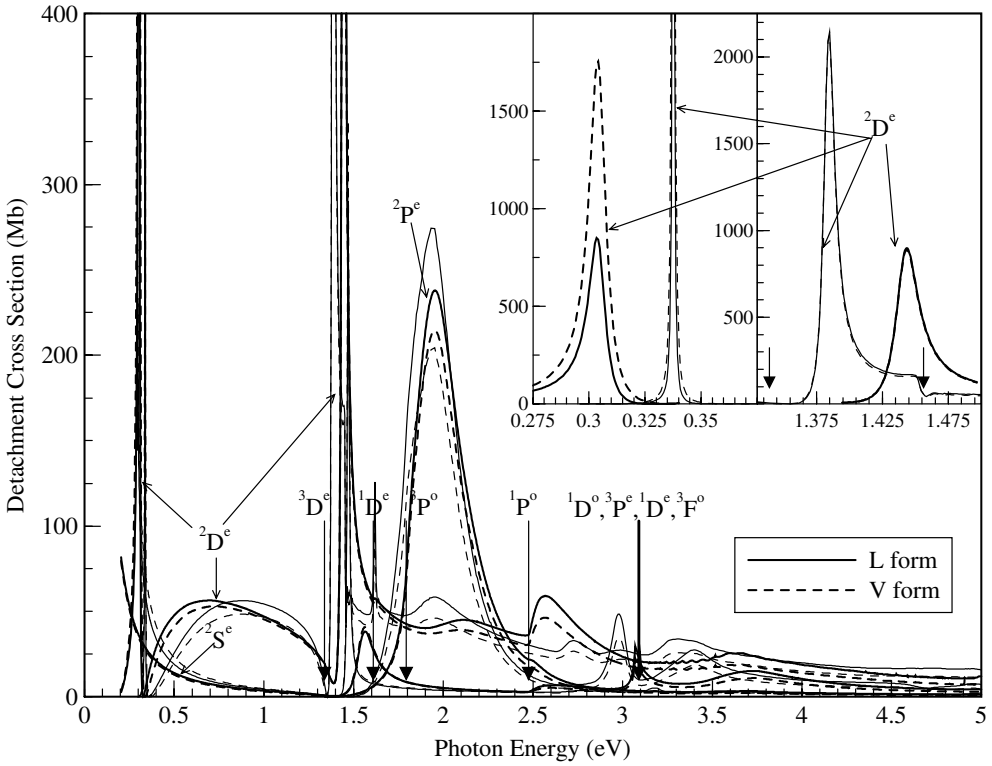

Figure 11. Detailed contributions of the three partial waves to the total photodetachment cross sections of Ba^- ions. The meanings of the curves are the same as in figure 5.

just above the threshold. The width of these resonance structures is apparently larger than that in the scattering cross section. An apparent quantitative difference between the CV and VO results can also be found around the peak between 1.8 and 2.2 eV. The disagreement above the 2.5 eV is mainly due to the positions of the four excitation thresholds from $^1P^o$ to $^3F^o$, which are given by the CV and VO calculations with a largest distance of 0.1 eV. Combined with the difference of 0.11 eV in the ionization energy, a shift of about 0.2 eV for the structures can be induced.

Partial cross sections of the photodetachment cross sections of Ba^- ions are presented in figure 11. One can see that the two sharp peaks occurring around 0.3 and 1.45 eV have the ^2D characteristics. This is consistent with what one has found in figure 3, that two ^2D shape resonances occur just above the elastic threshold and the first excitation threshold. However, the structures caused by these two resonances in the photodetachment cross section are broader than those in the electron scattering cross sections. The first ^2D shape resonance has been predicted by many authors before [20, 22, 23], while the second ^2D shape resonance just above the ^3D threshold has not been mentioned before in the literature. The ^2P symmetry also produces a strong but broader peak between 1.5 and 2.5 eV.

The contributions of the major ionization channels to the three partial cross sections of Ba^- ions are plotted in figures 12–14. In figure 12, the ionization channels for the ^2S symmetry are presented. All the peaks in the energy region from 1.3 to 3.5 eV behave as typical resonance structures rather than the so-called threshold effect. The cross section of the

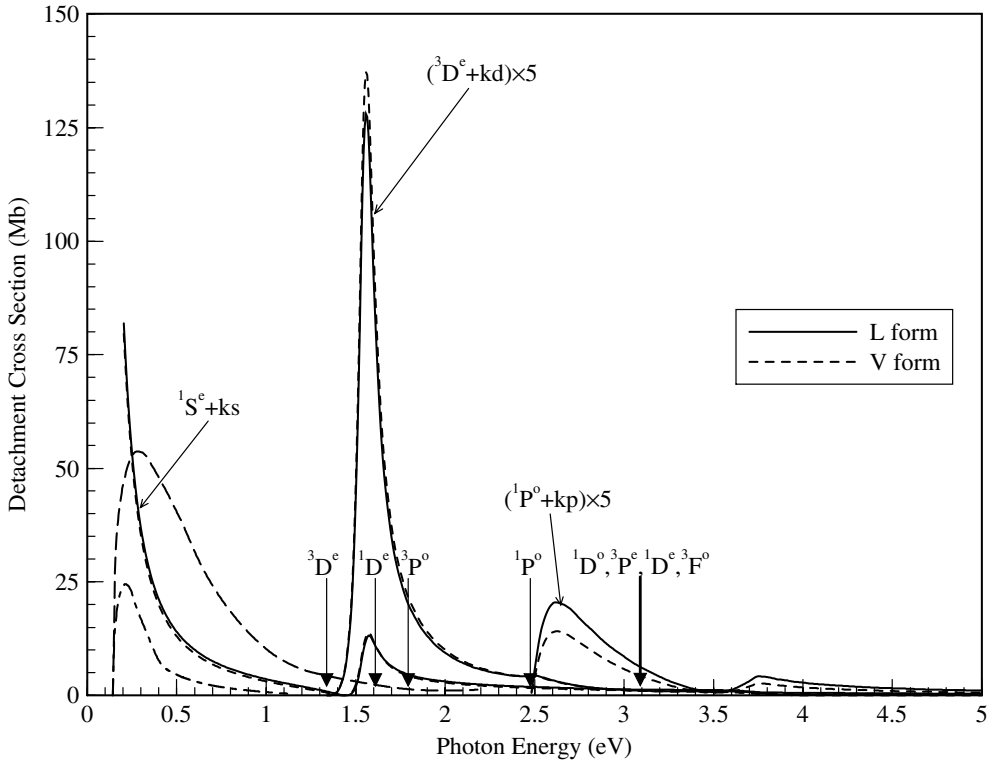

Figure 12. Detailed contributions of the individual ionization channels to the ^{2}S partial wave photodetachment cross sections of Ba^- ions. The meanings of the curves are the same as in figure 7.

^{2}S symmetry is dominated by three ionization channels, $(6s^2\ ^1S+ks)^2S$, $(6s5d\ ^2D+kd)^2S$, and $(6s6p\ ^1P^o+kp)^2S$. Contributions from other ionization channels are very small. In figure 12, the cross sections of the ionization channel $(6s^2\ ^1S+ks)^2S$ given by Gribakin *et al* [30] are plotted with a thick long-dashed curve for the length form and a thick dot–dashed curve for the velocity form. Quite large discrepancies exist between our results and theirs, and between the two forms of their result.

As follows from the inspection of figure 13, there are three strong ionization channels, which are $(6s5d\ ^3D+kd)^2P$, $(6s5d\ ^1D+kd)^2P$ and $(6s6p\ ^3P^o+kp)^2P$. One can expect interactions between these channels, resulting in interferences, as shown around 3.1 eV in this figure. From figure 14, it can clearly be seen that only channel $(6s^2\ ^1S+kd)^2D$ contributes to the first resonance peak below 0.32 eV, while all three channels, $(6s^2\ ^1S+kd)^2D$, $(6s5d\ ^3D+kd)^2D$ and $(6s5d\ ^3D+ks)^2P$, give comparable contributions to the photodetachment process. As the free electron energies are different for different ionization channels, the share of the total cross section among different channels relies on their interactions. As we did in figures 12 and14, the cross sections of the ionization channel $(6s^2\ ^1S+kd)^2D$ of Gribakin *et al* [30] are also plotted for comparison. For this ionization channel, the present result shows two zero cross section points. The first one is located at 0.33 eV just above the first ^{2}D shape resonance state, and the second one at 1.41 eV just above the ^{3}D excitation threshold. The result of Gribakin *et al* arrives at its zero cross section around 1.45 eV by the velocity form, and 1.65 eV by the length form. This is the only Cooper minimum point reached by their calculation. From the

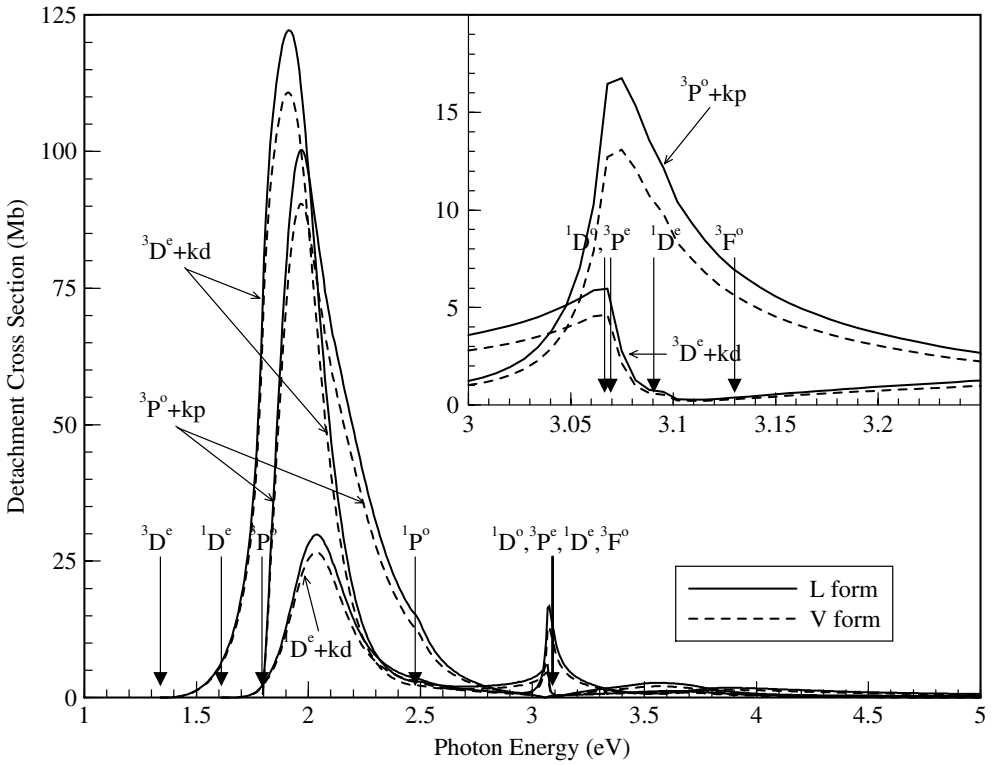

Figure 13. Detailed contributions of the individual ionization channels to the ^{2}P partial wave photodetachment cross sections of Ba^- ions. The meanings of the curves are the same as in figure 5.

elastic threshold to 1.5 eV, quite large discrepancies exist between our results and theirs, and between the two forms of their result.

In summary, we have carried out calculations on low-energy electron scattering from Sr and Ba atoms and the photodetachment of Sr^- and Ba^- ions by using the *R*-matrix method. Core–valence electron correlation has been shown to be very important to reproduce the experimental observations. The results for Sr clarify that the mini-peak observed in the early experiment is actually caused by the threshold effect on the elastic cross sections and the excitations to the first excited state, and that its correct position should be just above the first excitation energy. Results for the Ba atom show two ^{2}D shape resonance states: the first one is just above the elastic threshold and the second one just above the first excitation threshold of the ^{3}D state. Interactions between different ionization channels are reflected in the share of the photodetachment cross section among more than one ionization channel.

Acknowledgments

This work was supported by the National Science Fund for Distinguished Young Scholars under grant No 10025416, the National Natural Science Foundation of China under grant No 19974075, the National High-Tech ICF Committee in China and the Chinese Research Association of Atomic and Molecular Data.

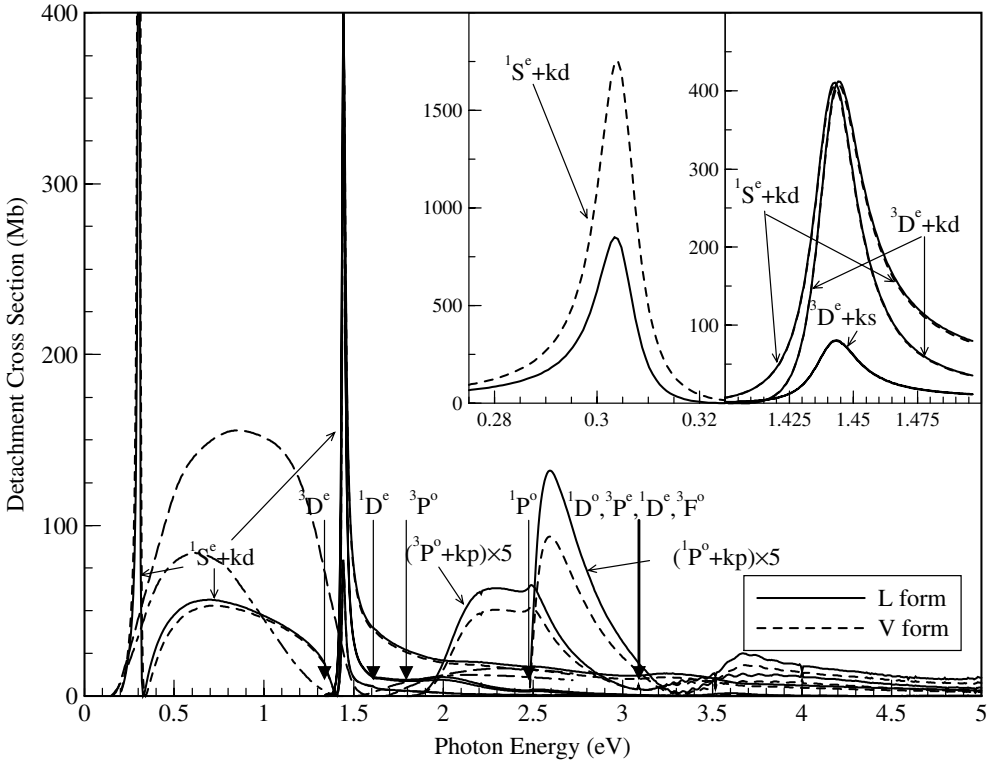

Figure 14. Detailed contributions of the individual ionization channels to the ^{2}D partial wave photodetachment cross sections of Ba^- ions. The meanings of the curves are the same as in figure 9.

References

[1] Pegg D J, Thompson J S, Compton R N and Alton G D 1987 *Phys. Rev. Lett.* **59** 2267
[2] Fischer C F, Lagowski J B and Vosko S H 1987 *Phys. Rev. Lett.* **59** 2263
[3] Fischer C F 1989 *Phys. Rev.* A **39** 963
[4] Kim L and Greene C H 1989 *J. Phys. B: At. Mol. Opt. Phys.* **22** L175
[5] Johnson W R, Sapirstein J and Blundell S A 1989 *J. Phys. B: At. Mol. Opt. Phys.* **22** 2341
[6] Gribakin G F, Gul'tsev B V, Ivanov V K and Kuchiev M Yu 1989 *Zh. Eksp. Teor. Fiz. Pis. Red.* **15** 32
[7] Fuentealba P, Savin A, Stoll H and Preuss H 1990 *Phys. Rev.* A **41** 1238
[8] Cowan R and Wilson M 1991 *Phys. Scr.* **43** 244
[9] Dzuba V, Flambuam F, Gribakin G F and Sushkov D 1991 *Phys. Rev.* A **44** 2823
[10] van der Hart H W, Laughlin C and Hansen J E 1993 *Phys. Rev. Lett.* **71** 1506
[11] Sundholm D 1995 *J. Phys. B: At. Mol. Opt. Phys.* **28** L399
[12] Salomonson S, Warston H and Lindgren I 1996 *Phys. Rev. Lett.* **76** 3092
[13] Nadeau M-J, Zhao X-L, Garwan M and Litherland A 1992 *Phys. Rev.* A **46** R3588
[14] Petrunin V V, Andersen H H, Balling P and Andersen T 1996 *Phys. Rev. Lett.* **76** 744
[15] Fabrikant I I 1975 *Atomniye Protsessi* (Riga: Zinatne) p 80
[16] Fabrikant I I 1988 *Phys. Rep.* **159** 1
[17] Romanyuk N I, Shpenik O B and Zapesochyi I P 1980 *Pis. Zh. Eksp. Teor. Fiz.* **32** 472
[18] Kurtz H A and Jordan K D 1981 *J. Phys. B: At. Mol. Phys.* **14** 4361
[19] Amusia M Ya, Sosnivker V A, Cherepkov N A and Chernysheva L V 1985 *Zh. Tekh. Fiz.* **55** 2304
[20] Yuan Jianmin and Zhang Zhijie 1989 *J. Phys. B: At. Mol. Opt. Phys.* **22** 2751
Yuan Jianmin and Zhang Zhijie 1990 *Phys. Rev.* A **42** 5363
Yuan Jianmin 1995 *Phys. Rev.* A **52** 4647

[21] Johnston A R, Gallup G A and Burrow P D 1989 *Phys. Rev.* A **40** 4770
[22] Gribakin G F, Gul'tsev B B, Ivanov V K, Kuchiev M Yu and Tančić A R 1992 *Phys. Lett.* A **164** 73
[23] Dzuba V A, Flambaum V V and Sushkov O P 1991 *Phys. Rev.* A **44** 4224
[24] Szmytkowski R and Sienkiewicz J E 1994 *Phys. Rev.* A **50** 4007
[25] Kelemen V I, Remeta E Yu and Sabad E P 1995 *J. Phys. B: At. Mol. Opt. Phys.* **28** 1527
[26] Heinicke E, Kaiser H J, Rackwits R and Feldmann D 1974 *Phys. Lett.* A **50** 265
[27] Walter C W and Peterson J R 1992 *Phys. Rev. Lett.* **68** 2281
Peterson J R 1992 *Aust. J. Phys.* **40** 293
[28] Kristensen P, Brodie C A, Pedersen U V, Petrunin V V and Andersen T 1997 *Phys. Rev. Lett.* **78** 2329
[29] Lee D H, Pegg D J and Hanstorp D 1998 *Phys. Rev.* A **58** 2121
[30] Gribakin G F, Gul'tsev B V, Ivanov V K and Kuchiev M Yu 1990 *J. Phys. B: At. Mol. Opt. Phys.* **23** 4505
[31] Yuan Jianmin 1999 *Abstracts of 21st. Int. Conf. on Physics of Electronic and Atomic Collisions (Sendai)* vol 1 p 121
[32] Fischer C F and Hansen J E 1991 *Phys. Rev.* A **44** 1559
[33] Yuan Jianmin and Fritsche L 1997 *Phys. Rev.* A **55** 1020
Yuan Jianmin 2000 *Phys. Rev.* A **61** 012704
[34] Yuan Jianmin and Lin C D 1998 *Phys. Rev.* A **58** 2824
[35] Burke P G, Hibbert A and Robb W D 1971 *J. Phys. B: At. Mol. Phys.* **4** 153
[36] Berrington K A, Eissner W B and Norrington P H 1995 *Comput. Phys. Commun.* **92** 290
[37] Hibbert A 1975 *Comput. Phys. Commun.* **9** 141
[38] Scott M P, Burke P G and Bartschat K 1998 *Photonic, Electronic and Atomic Collisions* (Singapore: World Scientific) p 229
[39] Moore C E (ed) 1970 *Atomic Energy Levels* NBS Title Series no I (Washington, DC: US Government Printing Office) p 242
[40] Palenius H P 1976 *Phys. Lett.* A **56** 451
[41] Friedrich H 1990 *Theoretical Atomic Physics* (New York: Springer)
[42] Wang S, Trajmar S and Zetner P W 1994 *J. Phys. B: At. Mol. Opt. Phys.* **27** 1613